-RESEARCH PAPER-

International Journal of Mining and Geo-Engineering

IJMGE

IJMGE 56-3 (2022) 225- 230

DOI: 10.22059/IJMGE.2022.320175.594898

Using the mass-radius method to quantify the disturbed zones in Sidi Chennane mine through geo-electrical images

Abderrahim Ayad [a, *], Saad Bakkali [a]

[a] *Earth Sciences Department, Faculty of Sciences and Techniques, Abdelmalek Essaâdi University, Tangier, Morocco.*

Article History:

Received: 09 March 2021.

Revised: 29 January 2022.

Accepted: 01 February 2022.

ABSTRACT

This paper presents a new approach to quantifying the rate of the disturbances within the phosphate series in an area of 50 hectares located in the Sidi Chennane deposit, Ouled Abdoun, Morocco. The proposed approach consists in applying the mass-radius fractal method on the geo-electrical images to estimate the fractal dimension FD as an index of the rate of the disturbances. The result of this study shows a strong correlation between the measured disturbed surfaces displayed on the studied geo-electrical images and their corresponding fractal dimensions. The calculated FD's values were found in the range of 2.081 to 2.719 and correspond to the range of the disturbances rates of 4.1 % to 17.7 % respectively. Therefore, the highest fractal dimension values reveal a high rate of disturbances and vice-versa. This analysis has confirmed that the fractal dimension may offer significant implications for distinguishing between the phosphate deposit at high disturbances rate and the deposit at low disturbances rate. This may lead to important implications for the mining engineers to obtain an accurate phosphate reserve estimate and make the best exploration and exploitation planning in the Sidi Chennane mine.

Keywords: *Disturbances, Fractal geometry, Geo-electrical image, Phosphate mine, Ouled Abdoun.*

1. Introduction

Morocco holds more than 75% of the world's phosphate reserves (50 000 billion metric tons). These considerable reserves were explored by the l'Office Chérifien des Phosphates (OCP) since the 1920s. The large extraction intensity since the 1920s allows Morocco to become the world's leading producer of phosphate with an annual output mining capacity of over 32 million tons [1, 2].

These important reserves were deposited in four sedimentary basins namely, Ouled Abdoun, Gantour, Meskala, and Boukraa (Figure.1). About 75% of these reserves exist in the Ouled Abdoun basin located in the central part of Morocco, about 200 km from the capital Rabat. This basin encompasses about 4500 km^2, containing at least 26.8 billion tons of phosphate. It is also the oldest exploited Moroccan phosphate basin, and the most important, both in terms of quality and quantity of phosphate [3].

This study focused on the Sidi Chennane mine which is one of the most important Moroccan phosphate mines, located in the northwest part of the Ouled Abdoun basin, near the city of Khouribga (Figure.1).

In the Sidi Chennane mine, the phosphate series is composed of several phosphate layers alternating with argillaceous, calcareous, and marly interlayers [4, 5]. The mining operation is done at an open pit [6], and the phosphate is separated from associated sterile materials (marls, limestones, silex, clays, etc.) by a combination of diverse processing stages involving crushing and screening, washing, and flotation [7].

The phosphate sequence of Sidi Chennane is frequently affected by disturbing bodies with a diameter varying from 10m to more than 150m, locally known as disturbances since they disturb the phosphate series regularity (Figure 2). These disturbing bodies are composed of an accumulation of phosphate limestone blocks with large nodules of marl, and some fragments of phosphate rock considered as waste rocky material that must be removed. The geological studies done in Sidi Chennane have shown that the origin of these disturbing bodies is related to a natural fall down caused by the dissolution of Senonian gypsum layers located under the phosphate sequence [8], other studies reveal that the origin of these bodies is supergene, even pedological [9]. The statistical studies of the investigated boreholes carried out in the Sidi Chennane mine revealed that out of 157 boreholes, 53 showed a "disturbed" phosphate series, i.e., 33% of the performed boreholes.

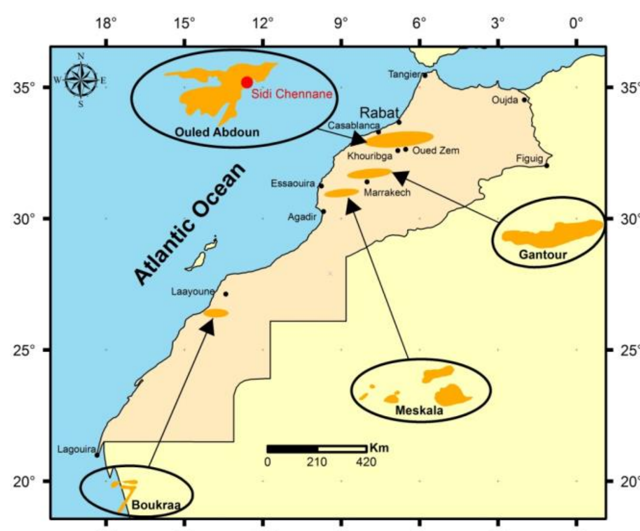

Figure 1. The main Moroccan phosphate basins, with the location of Sidi Chennane mine.

* Corresponding author. Tel: +2126003025199, *E-mail address:* abderrahim.ayad@etu.uae.ac.ma (A. Ayad).

During the exploration and exploitation stages, the existence of the disturbances causes serious problems. Firstly, as they are compact and hard, they disturb seriously the kinematic chain of the exploitation in some yards. For example, during the firing stage, the boring grids have to be tightened, so, the number of boreholes increases; thereby explosives and time-consuming increase drastically. Secondly, as we do not know the disturbing part hidden under the quaternary cover, the phosphate reserves estimations can be wrong. For these reasons, the quantification of the rate of the disturbances within the phosphate series is considered a crucial step and a challenging question for the OCP mining engineers.

Figure 2. Geological sections showing disturbed zone in Sidi Chennane mine.

The disturbances are ever found hidden under a quaternary cover (topsoil), and cannot be directly mapped using direct exploration methods such as surface geology or well logging. In light of this issue, geo-electrical prospecting methods were mainly used as appropriate tools able to image the disturbances and differentiate them from the phosphate rocks [10-12].

This work aims to quantify the disturbed areas displayed on the geo-electrical images using the fractal geometry invented by Benoît Mandelbrot in 1974 to describe objects of irregular and complex shapes [13, 14].

Fractal analysis was considered the revolutionized technology for various images which need proper processing to find out different problems. It was applied for describing image features like texture, roughness, smoothness, etc. for many objects on different length scales, extending from atomic size to gigantic size. Indeed, it is very interesting to provide a brief review of some fractal analysis applications. Only in recent years, has attention been paid to the advantages of using fractal geometry in remote sensing applications to measure the roughness or the textural complexity in images of land surfaces [15]; in the fractured surface application for the modeling of the spatial distributions of fracture networks in fractured rock bodies which is essential for the accurate understanding of the fluid flow within the rock mass [16-19]; in medical application to ensures the progress of the automatic diagnostic process to discriminate between healthy and unhealthy case [20-22]; and in urban geography issues, mainly in the description of urban morphologies (distribution of activities, built-up areas, borders, networks...), the settlement systems analysis and simulation of urban growth [23].

This paper aims to discuss the potential applicability of the mass-radius fractal method to quantify the rate of disturbed phosphate through geo-electrical images. It is an extension of previous work carried out using other fractal methods namely the box-counting method and the triangular prism surface area method, as well as the lacunarity and succolarity fractal methods [24-26]. This study would offer novel insights into the role of fractal dimension as a valuable addition to classical measures to obtain accurate phosphates reserves estimation and make the best exploration and exploitation planning.

2. Materials and Methods

2.1. The mass-radius method implementation

In this work, the fractal analysis was carried out using the mass-radius method sometimes referred to as the sandbox method [27]. The term mass-radius means the area measured using discs of increasing size. It is an easier tool in the calculation process and more effective to deal with irregular shapes. The typical approach of this method consists of placing in the center of the image to be measured a circular disc of increasing radius r. This generates a series of expanding concentric discs. Then at each radius size, the number of pixels contained in the disc is counted as M(r) (Figure.3).

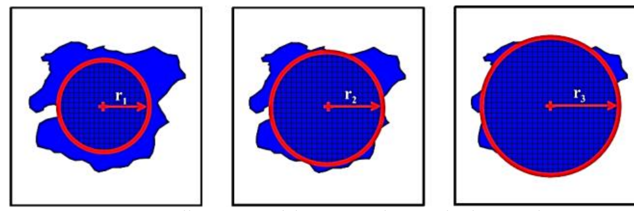

Figure 3. Illustration of the mass-radius method principle.

For an object in two-dimensional Euclidian space, the mass-radius is proportional to the square of the circle of radius r.

$$M(r) \propto r^2 \quad (1)$$

The set data obtained will be represented on a log-log Cartesian graph log M(r) versus log(r), which allows for identifying the fractal dimension FD from the slope of the straight line describing the graph:

$$FD = \frac{log(M(r))}{log(r)} \quad (2)$$

In this study, the fractal analysis was performed on 5151 geo-electrical data acquired from an area of 50 hectares located in the Sidi Chennane deposit.

2.2. Geo-electrical survey

According to [28], there are strong resistivity contrasts between the normal phosphate rock and the disturbances. Hence, the geo-electrical prospection had been mainly used as an excellent parameter and marker for the disturbed areas. The principal advantages of this method are its quick application and simple qualitative interpretation of the results.

In total, 51 geoelectrical profiles at a spacing of 20m were executed. There were 101 stations at a 5m distance for every profile, which makes 5151 measurement stations in the survey (Figure.4) [29].

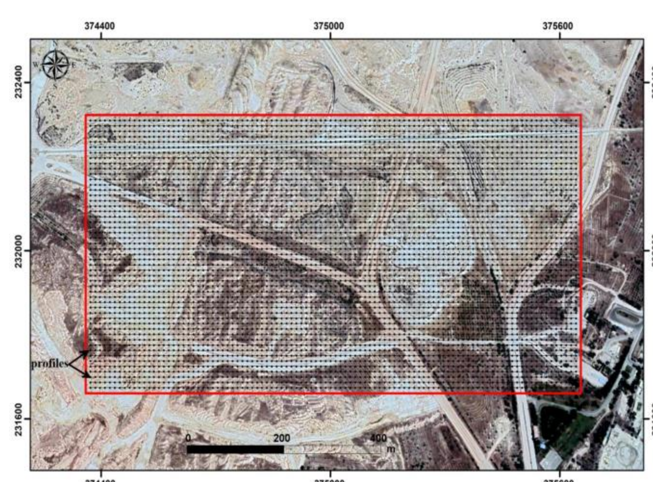

Figure 4. Geographic map showing the location of the geo-electrical profiles. The study area delimited by a red rectangle is currently under exploitation.

The acquired data were then interpolated and imaged in a 2D plan in order to define the anomalous areas corresponding to disturbances (Figure 5). Based on the geo-electrical image shown in Figure 5, it was found that normal phosphate rock has a resistivity range from 80 to 150 Ω.m, while the disturbances feature resistivity values range from 200 to 1000 Ω.m. This apparent resistivity contrast allows distinguishing between the phosphate series and the anomalous regions corresponding to disturbances. The high values of apparent resistivity corresponding to disturbances were encountered with a red circle in the image below (Figure.4).

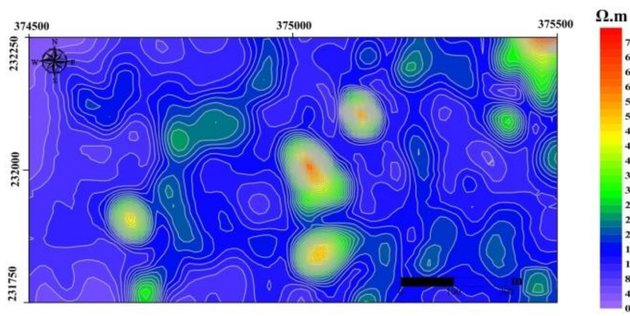

Figure 5. Result of geo-electrical mapping. The disturbed areas are surrounded by red circles.

2.3. Fractal analysis of the geo-electrical images

To perform a comparative fractal analysis, eight geo-electrical images were created from the original image using a cutoff frequency $\upsilon_{a.r}$ of 20Ω.m as shown in Figure 6. This allows showing how the disturbed surface extended from one image to another. Afterward, the geo-electrical images will be processed by fractal analysis using the mass-radius method to quantify the disturbed phosphate zones.

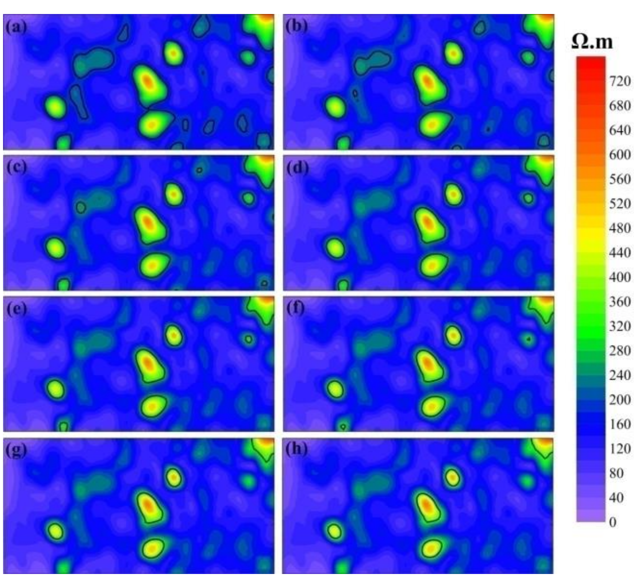

Figure 6. Geo-electrical images showing the spatial distribution of the disturbances over the study area. The cutoff frequencies $\upsilon_{a.r}$ used of each image are: (a) $\upsilon_{a.r}$=200Ω.m, (b) $\upsilon_{a.r}$=220Ω.m, (c) $\upsilon_{a.r}$=240Ω.m, (d) $\upsilon_{a.r}$=260Ω.m, (e) $\upsilon_{a.r}$=280Ω.m, (f) $\upsilon_{a.r}$= 300Ω.m, (g) $\upsilon_{a.r}$= 320Ω.m, (h) $\upsilon_{a.r}$= 340Ω.m.

Before starting the analysis process, the geo-electrical images have to be transformed into grayscale binary images (BMP format) in order to be adapted to the fractal analysis software requirement. A total of 8 black and white images of 510 by 255 pixels in size were produced, where the black pixels correspond to disturbances while the white pixels correspond to the phosphate rocks (Figure 7).

As we are working only on the disturbances, we can most likely leave sedimentary phosphates rocks out of our interpretation and constraint only on the disturbed areas. The obtained images show a view of the geometric forms of disturbed areas' boundaries. Then, for each black and white image, the surface of the disturbances was explored using the mass-radius method.

The fractal analysis investigation was carried out using a commercial computer program called Benoit™ (Version 1.3) from True Soft International (http://www.trusoft-international.com/benoit.html) [30]. Benoit™ is a computer program that enables measuring the fractal dimension using different methods such as the mass-radius method used in this work. This program is widely used in disciplines as diverse as geology, physics, medicine, and so on [31-33].

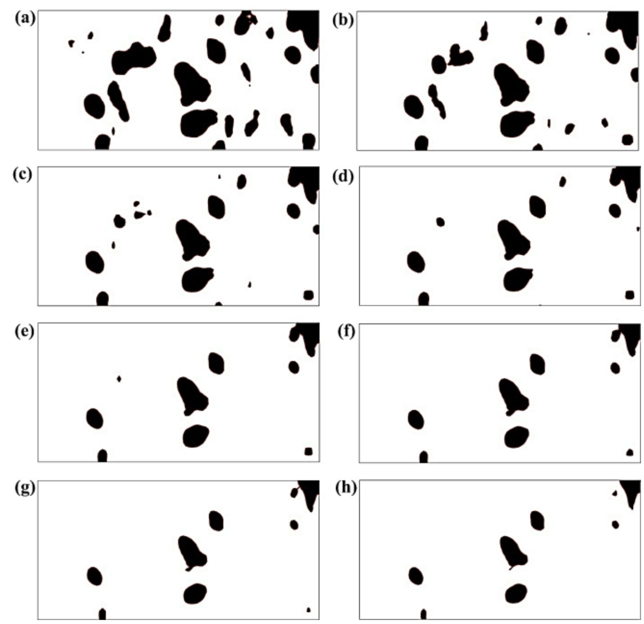

Figure 7. Black and white images version of the images in Figure 6.

3. Results and Discussion

Fractal dimensions (FD) of images in Figure 7 were determined using the mass-radius method. It is to note that the result obtained from the proposed method mainly refers to the number of circles used to sample the texture pattern under analysis, for the reason that after a given number of spheres, the texture is oversampled, i.e., no important information is added by each additional sphere. Another important parameter that can influence the results obtained by the proposed method is the number of pixels used to compute the texture pattern within an image.

The selected images were covered with circles of various radius r, and the number of pixels inside the circles was competed using Benoit 1.3 software. Afterward, a log-log graph was plotted (log M(r)-log(r)) which shows a linear character of the relationship between the circle radius size and the number of pixels contained within the radius. This is highlighted by the correlation coefficient R^2, which is found always above a value equal to 0.99. The plot (log M(r)-log(r)) produced a straight line with a slope equal to FD according to the number of spheres used during the sampling step. The results yielded are presented in Figure 8. The estimated FDs of different images yielded slightly different results, introducing some minor variations in the numerical values.

To validate the obtained FD's values and achieve a relevant classification of the studied images, as well as get an overall understanding of how these values vary as a function of the disturbances rate. The disturbed surface was measured (in m^2) using a geographic information system (GIS). Afterward, the estimated FD's values were correlated with the corresponding disturbances rates (Table 1). This was used to easily illustrate the proportionality between the disturbances rate in each image and the corresponding FD value.

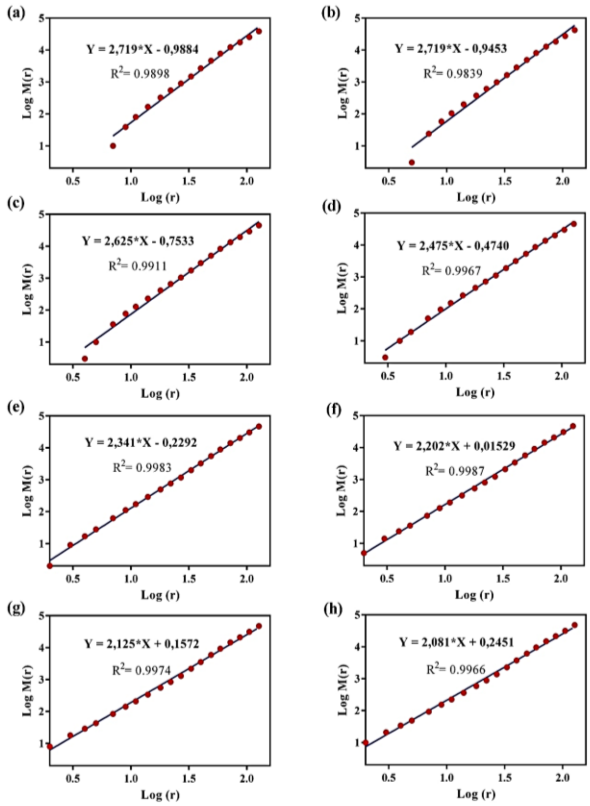

Figure 8. Benoit FD's outputs of the grayscale binary images displayed in Figure 7. (a) $\upsilon_{a.r}$=200Ω.m, (b) $\upsilon_{a.r}$=220Ω.m, (c) $\upsilon_{a.r}$=240Ω.m, (d) $\upsilon_{a.r}$=260Ω.m, (e) $\upsilon_{a.r}$=280Ω.m, (f) $\upsilon_{a.r}$= 300Ω.m, (g) $\upsilon_{a.r}$=320Ω.m, (h) $\upsilon_{a.r}$=340Ω.m.

From table 1 above, we observe that the FD's value grows constantly as a function of the disturbances rate. The FDs calculated are in the range 2.081-2.719 and correspond respectively to the disturbance rates range from 4.1 % to 17.7 %. The estimated FD values are the result of one of the main contributions to the image complexity, that is the space-filling effect of the image interior. It appears that the FD's values were influenced by the surface occupied by the disturbances in the overall studied area. This correlation provides proof to support the idea that a fractal dimension is a measure of space-filling. Hence, the highest FDs' values indicated that the disturbances filled more space and viscera.

Having in mind the obtained results, the fractal analysis mass-radius method used in this work is simple enough to be appropriate for a complete understanding of the extent of the disturbance within overall the study area. Our results reinforce the idea that the FD values can be an objective and useful parameter to characterize the disturbances. This may become a proper tool to consistently get an accurate diagnosis to distinguish the phosphate deposit of low rates and the deposit of high rates of disturbances. Finally, we propose that the FD values of disturbed phosphate deposits may be used, in addition by the mining engineers as a kind of guide to planning mining operations.

4. Conclusion

Throughout this work, we studied the utility of the mass-radius method as a new fractal approach to discriminate between the phosphate deposit at high risk of disturbances and the deposit at low risk via geo-electrical images. The work was carried out in an area of 50 hectares located in the Sidi Chennane deposit, Ouled Abdoun, Morocco.

First, the paper summarizes and synthesizes the research work concerning the disturbances, their origins, their spatial distributions, their detection methods, and their impacts during the exploration and exploitation stages. Then, a brief review of the fundamentals of fractal geometry was also discussed. The paper also brings the principle and the methodological framework of the mass-radius method, including the mathematical formulas by which it is calculated.

Table 1: Correlation of the estimated FDs with their corresponding disturbances rate.

Geo-electrical image	The surface of phosphate (m²)	The surface of disturbances (m²)	disturbances rate (%)	FD
$\upsilon_{200\Omega.m}$	411581	88419	17.70	2.719
$\upsilon_{220\Omega.m}$	438598	61402	12.30	2.719
$\upsilon_{240\Omega.m}$	455202	44798	8.96	2.625
$\upsilon_{260\Omega.m}$	462855	37145	7.43	2.475
$\upsilon_{280\Omega.m}$	468179	31821	6.40	2.341
$\upsilon_{300\Omega.m}$	472097	27903	5.60	2.202
$\upsilon_{320\Omega.m}$	475943	24057	4.81	2.125
$\upsilon_{340\Omega.m}$	479477	20523	4.10	2.081

The fractal analysis was performed on eight grayscale binary images, producing results of practical significance supported by the positive correlation between the estimated rate of disturbances and the corresponding fractal dimension. Hence, through this work, the fractal approach proves its significance and seems to be most appropriate to quantify, compare, and evaluate the disturbed phosphate deposit. This may lead to an interesting assumption about using the fractal geometry tools as an important addition to classical methods to get accurate phosphate reserve estimation and make the best exploration and exploitation planning.

Since the fractal analysis seems simple enough and provides more convincing results, it paves the way for promising future studies; in particular, the use of 3D fractal analysis could better characterize the texture of the disturbances in depth. However, it is possible to use some analytical methods, such as the cube-counting method derived from the box-counting method [34, 35].

Acknowledgments

The author thanks the Chief Editor, handing Editor, and the anonymous reviewers for their critical comment and their helpful recommendations.

REFERENCES

[1] Walana, P., Davidssona, S., Johansson, S., Höök, M. (2015). Phosphate rock production and depletion: Regional disaggregated modeling and global implications. Resources Conservation and Recycling, (93), 178–187. http://dx.doi.org/10.1016/j.resconrec.2014.10.0111.

[2] Azmany, M., Farkhany, X., & Salvan, H.M. (1986). Gisement des Ouled Abdoun, Géologie des Gîtes Minéraux Marocains. Notes et Mémoires, Service Géologique du Maroc, 276(3), 200-249.

[3] Edixhoven, J. D., Gupta, J., & Savenije, H. H. G. (2014). Recent revisions of phosphate rock reserves and resources: a critique. Earth System Dynamics, (5), 491–507. https://doi:10.5194/esd-5-491-2014

[4] El Haddi, H., Benbouziane, A., Jourani, E., Amaghzaz, M., & Mouflih, M. (2011). La silicification des phosphates marocains: Typologie génétique et conséquences industrielles". 1st International symposium on innovation and technology in phophate industry (Symphos), Marrakech-Morocco, 111-112.

[5] Moutaouakil, D., & Giresse, P. (1993). Pétrologie et environnement sédimentaires des phosphates méso-cénozoïques du bassin des Oulad Abdoun (Maroc). Bulletin de la Société Géologique de France, (164), 473–491.

[6] Daafi, Y., Chakir, A., Jourani, E., Ouabba., S.M. (2014). Geology and mine planning of phosphate deposits: Benguerir deposit Gantour Basin – Morocco. Procedia Engineering, (83), 70 – 75. https://doi.org/10.1016/j.proeng.2014.09.014

[7] Hakkou, R., Benzaazouab, M., Bussière, B. (2016). Valorization of phosphate waste rocks and sludge from the Moroccan phosphate mines: Challenges and perspectives. Procedia Engineering, (138), 110 –118. https://doi.org/10.1016/j.proeng.2016.02.068

[8] Kchikach, A., Jaffal, M., Aïfa, T., & Bahi, L. (2002). Cartographie de corps stériles sous couverture quaternaire par méthode de résistivités électriques dans le gisement phosphaté de Sidi Chennane (Maroc). Comptes Rendus Géoscience, 334(6), 379-386. https://doi.org/10.1016/S1631-0713(02)01767-4

[9] Boujo, A. (2002). About shape and development of sterile bodies in phosphatic deposits. Comptes Rendus Geoscience, 334(16), 1113-1114.

[10] Kchikach, A., Andrieux, P., Jaffal, M., Amrhar, M., Mchichi, M., Boya, B., Amaghzaz, M., Veyrieras, T., & Iqizou, K. (2006). Les Sondages Électromagnétiques Temporels Commeoutil de Reconnaissance du Gisement Phosphaté de Sidi Chennane (Maroc): Apport à la Résolution d'un Problème D'Exploitation. Comptes Rendus Geoscience, 338, 289-296. https://doi:10.1016/j.crte.2006.02.003

[11] Baba, K., Bahi, L., Ouadif, L., & Akhssas, A. (2012). Mapping sterile bodies in the sidi chennane phosphatic deposit (Morocco) using geoelectrical investigations. International Journal of Engineering Research and Applications, (2), 2132–2136.

[12] El Assel, N., Kchikach, A., Teixidó, T., Peña, J.A., Jaffal, M., Guerin, R., Lutz, P., Jourani, E.S., Amaghzaz, M. (2011). A Ground Penetrating Radar and Electrical Resistivity Tomography Prospection for Detecting Sterile Bodies in the Phosphatic Bearing of Sidi Chennane (Morocco). International Journal of Geosciences, (2), 406-413. https://doi:10.4236/ijg.2011.24044

[13] Mandelbrot, B. (1967). How long is the coast of Britain? statistical self-similarity and fractal dimension. Science, 156, 636-638. https://doi.org/10.1126/science.156.3775.636

[14] Mandelbrot, B. (1975). Stochastic Models of the Earth's Relief, the Shape and the Fractal Dimension of the Coastlines, and the Number-area Rule for Islands. Proceedings of the National Academy of Sciences, 72(10), 3823-3828.

[15] Nie, Q., Shi, K., Gong, Y., Ran, F., Li, Z., Chen, R., Hua, L. (2020). Spatial-Temporal Variability of Land Surface Temperature Spatial Pattern: Multifractal Detrended Fluctuation Analysis. IEEE Journal of Selected Topics in Applied Earth Observations and Remote Sensing, 13, 2010-2018. https://doi.org/10.1109/JSTARS.2020.2990479

[16] Kovács, D., Dabi, G., & Vásárhelyi, B. (2019). Image processing for fractal geometry-based discrete fracture network modeling input data: A methodological approach, Central European Geology, 62(1), 1-14. https://doi.org/10.1556/24.61.2018.09

[17] Liu, X., Liang, T., Wang, S., Nawnit, K. (2019). A Fractal Model for Characterizing Hydraulic Properties of Fractured Rock Mass under Mining Influence. Geofluids, 2019, 17. https://doi.org/10.1155/2019/8391803

[18] Wei, W., Xia, Y. (2017). Geometrical, fractal and hydraulic properties of fractured reservoirs: A mini-review. Advances in Geo-Energy Research, 1(1), 31-38. https://doi.org/10.26804/ager.2017.01.03

[19] Jorge, A.L., Luis, H.O., & Jerson, A.G. (2016). Identification of natural fractures using resistive image logs, fractal dimension and support vector machines. Ingeniería e Investigación, 36(3), 125-132. http://dx.doi.org/10.15446/ing.investig.v36n3.56198

[20] Marusina, M. Y. and Karaseva, E. A. (2019). Automatic Analysis of Medical Images Based on Fractal Methods. International Conference. Quality Management, Transport and Information Security, Information Technologies, 349-352, https://doi.org/10.1109/ITQMIS.2019.8928378

[21] Elblbesy, M. A., Attia. M. (2020). Optimization of fractal dimension and shape analysis as discriminators of erythrocyte abnormalities. A new approach to a reproducible diagnostic tool. Mathematical Biosciences and Engineering, 17(5), 4706-4717. https://doi.org/10.3934/mbe.2020258

[22] Sun, T., Wang, X., Lin, D., Bao, R., Jiang, D., Ding, B., & Li, D. (2021). Medical image security authentication method based on wavelet reconstruction and fractal dimension. International Journal of Distributed Sensor Networks, 17(4). https://doi.org/10.1177/15501477211014132

[23] Chen Y. (2020). Fractal Modeling and Fractal Dimension Description of Urban Morphology. Entropy (Basel, Switzerland), 22(9), 961. https://doi.org/10.3390/e22090961

[24] Ayad, A., Amrani, M., & Bakkali, S. (2019). Quantification of the disturbances of phosphate series using the box-counting method on geoelectrical images (Sidi Chennane, Morocco). International Journal of Geophysics, 1-12. https://doi.org/10.1155/2019/2565430

[25] Ayad, A., & Bakkali, S. (2019). Fractal assessment of the disturbances of phosphate series using lacunarity and succolarity analysis on geoelectrical images (Sidi Chennane, Morocco). Complexity, 1-12. https://doi.org/10.1155/2019/9404567

[26] Ayad, A. & Bakkali, S. (2018). Assessment of the geoelectrical anomalies of the disturbances of phosphate series using the triangular prism surface area method (sidi chennane -Morocco). Proceedings of the 2nd Conference on Geophysics for Mineral Exploration and Mining, Porto, Portugal, (2018), 1-5. https://doi.org/10.3997/2214-4609.201802743

[27] Witten, T.A., & Sander, L. M. (1981). Diffusion-limited aggregation is a kinetic critical phenomenon. Physical Review Letters, 47, 1400-1403. https://doi.org/10.1080/001075100409698

[28] Bakkali, S., (2006). A resistivity survey of phosphate deposits containing hardpan pockets in Oulad Abdoun, Morocco. Geofisica Internacional, 45(1), 73-82.

[29] Bakkali, S. (2007). Enhancement of edges of Sidi Chennane phosphate "disturbances" using sun shading responses of resistivity data. Russian Geology and Geophysics, 48(9), 775-781. https://doi.org/10.1016/j.rgg.2006.12.012

[30] William, S. (1999). Order from Chaos. Science, 285 (5431).

[31] Mendoza-Ponce, A., Figueroa-Soto, A., Soria-Caballero, D., Garduño-Monroy, V. H. (2018). Active faults sources for the Pátzcuaro–Acambay fault system (Mexico): fractal analysis of slip rates and magnitudes Mw estimated from fault length. Natural Hazards and Earth System Sciences, 18, 3121–3135. https://doi.org/10.5194/nhess-18-3121-2018

[32] Huang, J. G., Christian, J. M., McDonald, G. S. (2018). Spontaneous spatial fractal pattern formation in dispersive systems. Journal of Nonlinear Optical Physics & Materials, 26(01). https://doi.org/10.1142/S0218863517500096

[33] Bianciardi, G., Sorce, F., Pontenani, A., Ginori, F., Scaramuzzino, S., & Tripodi. (2018). Fractal Approaches to Image Analysis in Oncopathology. Austin Journal of Medical Oncology, 5(2), 1-5

[34] Suzuki, M.T. (2007). A three-dimensional box-counting method for measuring fractal dimensions of 3D models. In Proceedings of the Eleventh IASTED International Conference on Internet and Multimedia Systems and Applications (IMSA '07). ACTA Press, USA, 42–47.

[35] Akkari, H., Bhouri, I., Dubois, P., Bedoui M.H.(2008). On the Relations Between 2D and 3D Fractal Dimensions: Theoretical Approach and Clinical Application in Bone Imaging. Mathematical Modelling of Natural Phenomena, 3 (6), 48-75. https://doi.org/10.1051/mmnp:2008081